From Data to Assessments and Decisions: Epi-Spline Technology*

Johannes O. Royset

Department of Operations Research
Naval Postgraduate School
joroyset@nps.edu

Roger J-B Wets

Department of Mathematics
University of California, Davis
rjbwets@ucdavis.edu

Abstract. Analysts in every field face the challenge of how to best use available data to estimate performance, quantify uncertainty, and predict the future. The data is almost never "just right," but rather scarce, excessive, corrupted, uncertain, and incomplete. External information derived from experiences, established "laws," and physical restrictions offer opportunities to remedy the situation and should be utilized. Applications in sustainable energy, natural resources, image reconstruction, financial planning, uncertain quantification, and reliability engineering are rich with problems where decisions rely on data analysis under such circumstances. We address these problems within a framework that identifies a function that according to some criterion best represents the given data set and satisfies constraints derived from the data as well as external information. Epi-splines provide the linchpin that allows us to handle shape restrictions, information growth, and approximations.

Keywords: splines, epi-splines, epi-convergence, epi-topology, financial curves, forecasting, regression, shape restriction, information fusion, constrained optimization

AMS Classification: 90C31, 90C48, 65K10, 65D15, 62G05

Date: January 8, 2014

*This material is based upon work supported in part by the U. S. Army Research Laboratory and the U. S. Army Research Office under grant numbers 00101-80683, W911NF-10-1-0246 and W911NF-12-1-0273, and, in part, was carried out while the first author was on a sabbatical leave at the University of California, Department of Mathematics. The authors also thank B. Chern, Stanford University, S. Ryan, Iowa State University, D. Singham, NPS, J.-P. Watson, Sandia Laboratory, and D. Woodruff, UC Davis, for providing information about epi-spline applications.

1 Introduction

Much of operations research and management science practice centers on utilizing available data to gain insight about a phenomenon, predict future performance, and instantiate optimization and simulation models. The process intersects several disciplines. Computer scientists refer to it as "learning." Statisticians talk about "data analysis," "regression," and "inference." At a fundamental level, the process relates to function approximation theory of mathematics, which has a long and prestigious history. Initially, polynomial-type approximations and generalized Fourier series were the mainstay of approximation theory both at the theoretical and computational levels. With the advent of digital computers, piecewise polynomials in the form of splines became computationally tractable and offered the possibility of much more accurate and stable approximations.

Although data receives the primal attention, at least in theoretical studies, information about an underlying phenomenon derives from a much wider range of sources. Data is never obtained in a vacuum, but rather in a context that provides *external information* in a variety of ways. Physical laws about the phenomenon may dictate that a regression line is increasing. Asymptotic theory could indicate that a probability density function is "nearly" normal. An analyst's experience gives a host of "soft" information, may be about ranges of possible values, signs of correlations, and number of modes. It is essential, especially when the data is limited, corrupted, and otherwise deficient, to utilize *all* available information, both from data and external sources. This is intuitively understood and widely exploited in practice. However, the theoretical foundation and computational tools for carrying out this process are incomplete. In this tutorial, we describe recent efforts to remedy the situation through the formulation of optimization problems and the examination of such problems via variational analysis. Specifically, we address the problem of how to

identify a function that best represents data and also satisfies information-driven constraints.

The problem arises broadly in curve fitting, interpolation, regression, density estimation, and numerous other contexts. In §2, we describe applications in the financial and commodity markets, and list several others. Numerical examples are given in §6. The information-driven constraints are formulated based on external information as well as the data, and come in a multitude of forms as illustrated below. The "best" is quantified by a criterion that could be least-squares, maximum likelihood, minimum error measure, etc. We refer to this problem as the *functional identification problem (FIP).*

The generality of FIP and its central position in a wide array of quantitative fields give rise, naturally, to a truly immense literature on the subject. We make no attempt to present a comprehensive treatment, but instead offer a biased view grown out of our gradual realization of the central role of variational analysis in problems of this kind. We formulate FIP as a constrained infinite-dimensional optimization problem that represent a *true* underlying problem. Incomplete information and simplifications introduced for computational reasons lead to *approximate* optimization problems. These problems are subsequently solved by standard, or possibly specialized, optimization algorithms to obtain best fits,

estimates, and approximations. We then rely on variational analysis to examine whether the solutions of the approximate problems are indeed approximations of solutions of the true problem, study associated convergence rates, and obtain other insights.

Since determining an arbitrary function requires pinning down an infinite number of parameters, an unavoidable simplification comes from replacing such functions by simpler ones that are fully characterized by a finite number of parameters. The consideration of simple, but hopefully representative, functions is of course common in linear regression, parametric density estimation, interpolation, and many other areas. *Epi-splines* are newly developed piecewise polynomial functions, described by a finite number of parameters, that are exceptionally flexible. In fact, epi-splines approximate essentially any function one can reasonably expect to encounter in practice, including those with discontinuities, unbounded derivatives, and even the function values $-\infty$ and ∞. We provide an introduction to epi-splines and their many applications; see [21, 20, 22] and reference therein for further details.

The remaining of the overview is organized as follows. §2 provides a glimpse of the many applications served by epi-spline technology. The mathematical formulation of FIP and definition of epi-splines are given in §3. The examination of FIP relies on variational analysis, with pertinent facts reviewed in §4. §5 summarizes theoretical results that justify the application of epi-spline technology. The tutorial ends in §6 with numerical examples.

2 Applications

Despite their recent discovery, epi-splines are applied in numerous areas. The first explicit use of epi-splines, under the name epi-curves, was in the context of deriving the zero-curves associated with a family of financial instruments [28, 27]; EpiRisk Research used it to build interest rates and currency exchange models and this has now also been packaged by independent software providers. In the energy domain, epi-splines are used to compute day-ahead forecasts of electricity (load) demand [13, 16]. In fact, there epi-splines are the main tools for building a stochastic process that not only provide a point forecast, but conditional distributions of demand for a 24-hour period. The situation is similar in forecasting of commodity prices, where epi-splines result in remarkably accurate estimates of copper prices [29]. Epi-splines are well-suited for probability density estimation, especially in the context of little data [7, 25, 21]. Uncertainty quantification and simulation output analysis are applications that directly benefit from the epi-spline technology for density estimation [19, 24]. Variograms are central tools in spatial statistics and preliminary tests show the promise of epi-splines also in that area [20].

Initial efforts on epi-splines centered on functions defined on a compact subset of the real line; see [20] for an overview. Although this covers many important applications, higher dimensions undoubtedly arise too. Initial efforts in image reconstruction [25, 22], density estimation [25, 22], response surface building [22], and graph models show the possibilities (§2.4). In this section, we provide a few examples that help motivate the analysis of FIP, with additional ones furnished by §6.

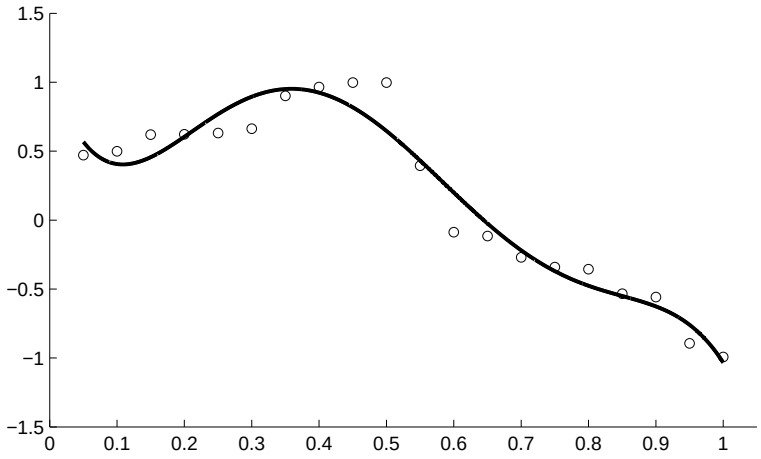

Figure 1: Curve fitting with polynomial of degree 5.

2.1 Curve Fitting

An elementary example from curve fitting highlights central components of FIP. Figure 1 illustrates 20 data points and plots a least-squares approximating 5th-degree polynomial. The polynomial fit is clearly too coarse, with polynomials of other degrees resulting in even worse approximations. This was early recognized and was a major motivation for the development of fitting procedures based on piecewise polynomials, specifically splines [23]. We fit the data relying on four such procedures. Each one assumes, implicitly, that the true function belongs to a particular family of functions and relies on a specific fitting criterion. The first three assume that the function is continuous whereas the last one allows for a potential discontinuity at $x = 0.525$. We begin by relying on common cubic spline fitting. The solid blue line in Figure 2 plots the cubic interpolating spline with the usual Lagrangian end conditions whereas the dashed black line is the least-squares cubic smoothing spline with smoothing penalty $1 \cdot 10^{-4}$ assigned to the second-order derivative term. The fits improve over the polynomial fit, though the "smoothness" of the smoothing spline curve depends on the choice of penalty.

The final two procedures rely on epi-splines built from second-degree polynomials. Suppose that in addition to the data, the analyst believes that the true function is continuously differentiable, with second-order derivatives in the range $[-100, 100]$. This external information forms constraints on the allowable functions that together with a least-squares criterion give the dashed black line in Figure 3. The epi-spline line resembles the smoothing spline of Figure 2, with the former having a slightly better fit at some points. The smoothing spline is a result of minimizing squared error *plus* a weighted integral of second-order derivatives. The epi-spline simply minimizes the squared error, but accounts for (pointwise) bounds on the second-order derivatives.

Suppose that external information further indicates that there may be a discontinuity around $x = 0.525$.

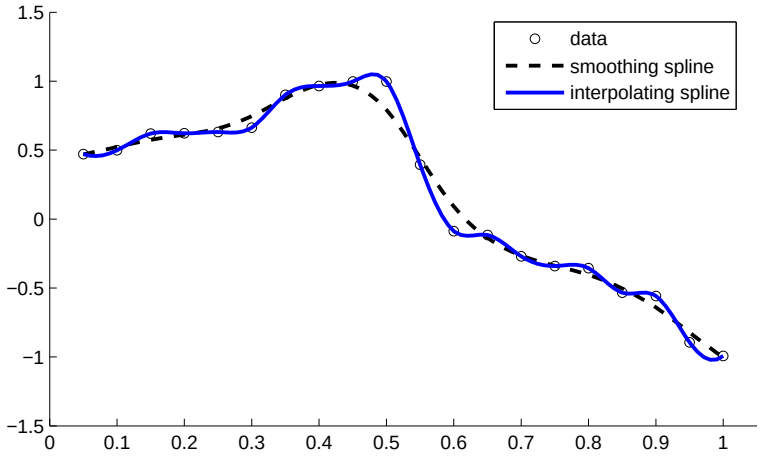

Figure 2: Cubic interpolating and smoothing spline fits.

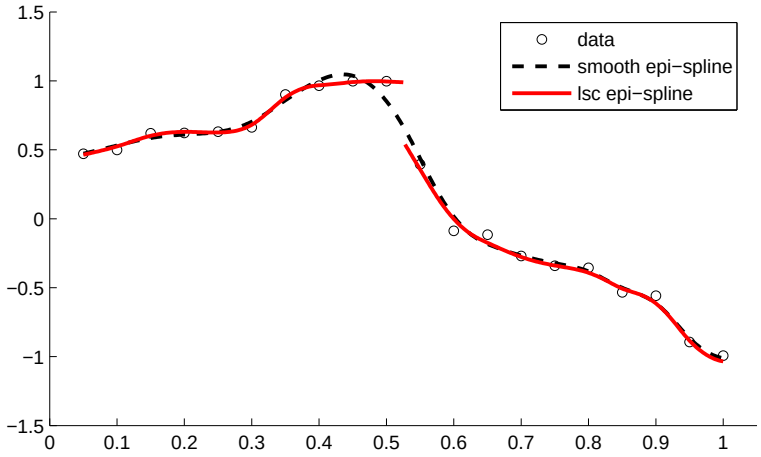

Figure 3: Second-order epi-spline fits with and without discontinuity.

Then an epi-spline illustrated by the solid red line in Figure 3 yields what appears to be the best fit seen so far. Although not pursued further here, other epi-splines could be calculated that satisfy additional constraints derived from external information about concavity and other jumps, or by collecting further data points. A sequence of such problems can be thought of as approximations of a "true" FIP involving an infinite number of data points and general functions. Below we discuss justifications for such approximations, especially those involving replacing general functions under consideration by epi-splines.

2.2 Financial Curves

It is standard procedure in financial engineering to use a family of similar instruments consisting of Treasury bonds, annuities, commercial papers and/or related assets to estimate their zero-curves including the spot rate curve, the forward rate curve, and the discount factor curve. These curves are intimately related as any one of them can be derived from knowing any one of the others; see [28, 27] and references therein. Here, we consider the problem of finding a discount factor curve d for the sake of illustration.

Suppose that for each instrument $i = 1, 2, ..., I$, there is a cash-flow yielding

$$\text{cash payments } p_0^i, p_1^i, \ldots, p_{N_i}^i \text{ at points in time } t_0^i, t_1^i, \ldots, t_{N_i}^i, \text{ respectively.}$$

The first one of these "payments" usually corresponds to purchasing price, the remaining ones to the income generated; so, p_0^i is usually negative whereas the remaining ones are positive. To simplify the notation, we let $t_0^i = 0$ (today) and $T \geq t_{N_i}^i$, for example related to the longest maturity time of all the instrument. Since one can reasonably assume that the discounted value of future payments balances the initial expense, or more generally the signed, discounted payment stream equals zero, identifying a discount factor curve comes down to finding a real-valued function d on $[0, T]$ with

$$\sum_{j=0}^{N_i} d(t_j^i) p_j^i = 0 \quad \text{for all } i = 1, 2, ..., I.$$

External information about the nature of discount factor curves dictates further that $d(0) = 1$ (the value of money today is its face value), $d \geq 0$ (discount factors are nonnegative numbers), and the derivative $d' \leq 0$ (discount factors cannot increase with time). Additional information that relates to the desirable properties of the associated forward rates curves, cf, [27, §1], justifies the restrictions to smooth curves and we therefore also require that d is continuously differentiable. Since ensuring that all of the above I equations are satisfied may not be possible due to inconsistent pricing in the markets, we formulate the problem in terms of a norm-minimizing optimization problem:

$$\text{minimize } \left\| \left(\sum_{j=0}^{N_1} d(t_j^1) p_j^1, ..., \sum_{j=0}^{N_I} d(t_j^I) p_j^I \right) \right\| \text{ such that } d(0) = 1,\ d \geq 0,\ d' \leq 0,$$

where it is implicitly assumed that d is a continuously differentiable function and $\| \cdot \|$ is a well-chosen norm. The problem is clearly a FIP, with constraints derived from insight about the situation.

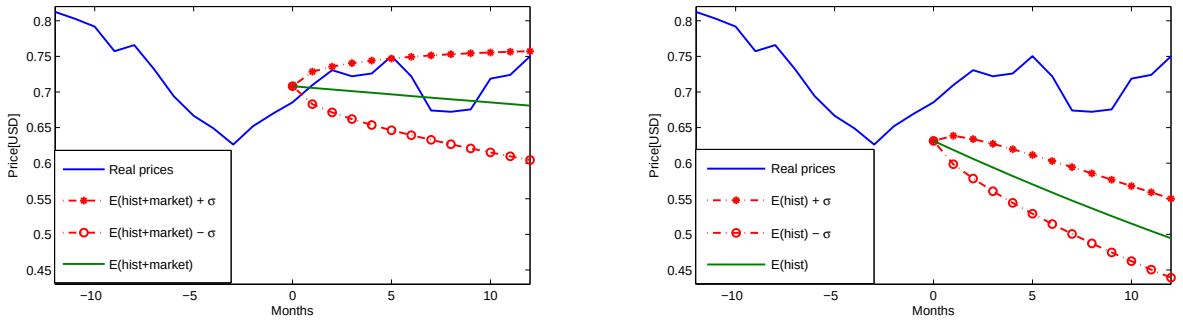

(a) (b)

Figure 4: Epi-spline estimates of copper prices with (a) and without (b) future contract information.

2.3 Commodity Price Forecasts

A more complicated example arises in commodity pricing. In [29, §3], epi-spline technology builds a stochastic process for short-term copper prices, say for the next 6-12 months. The effort relies on a common model for the evolution of copper prices as well as closely related quantities such as interest rates and exchange rates based on geometric Brownian motion. The drift and volatility terms in the corresponding stochastic differential equation, however, are estimated using epi-splines. The available information is historical prices, see for example the blue line in Figure 4(a), where "today" is month 0 so that prices only up to that time is available. Moreover, we also know current prices of future contracts for copper deliveries as well as for various interest rate and currency exchange instruments.

Epi-spline technology enters then twice. First, prices of future contracts are converted into (implied future) spot prices. This is achieved by computing a discount factor curve in the manner describe above and then converting it into a spot rate curve using standard expressions. Second, the historical prices, today's price, and the spot market prices just computed for, say, the next 9 months provide data that is fitted using a second-order epi-spline under the additional external information that it is continuously differentiable. The resulting fit provides estimated drift terms for the stochastic differential equation. The green line in Figure 4(a) shows the price drift for the next 12 months. We note that in this approach the initial conditions of the process is not today's observed price. A justification for proceeding in this fashion is that one should view today's (observed) spot price as the "actual" spot price perturbed by some noise; empirical calculations carried out in [29, §6.1] confirm that this approach yields much better results.

Finally, the volatility parameters of the process are obtained by a least-square fit of the covariance after adjusting the observed historical prices and the forecasted spot prices by subtracting their estimated expectation; for more about this approach cf. [29]. Figure 4(a) illustrates the volatility with dotted red lines corresponding to the 95% confidence interval for the process at each point in time. Figure 4(b) provides similar results, but without using epi-spline technology to convert information about

future contracts into implied future spot prices. It is apparent that including this additional external information dramatically improves the quality of the estimates.

2.4 Density Estimation on Graphs

A final illustration is provided by a problem in graph theory. There is a rapidly growing literature on models for graphs that rely on exponential families of probability density functions

$$h_\beta(G) = \exp\left(\sum_{i=1}^{I} \beta_i T_i(G) + c_\beta\right)$$

to describe the likelihood of a graph G characterized by its number of edges ($T_1(G)$), triangles ($T_2(G)$), stars ($T_3(G)$), cycles ($T_4(G)$), etc., with $\beta = (\beta_1, \beta_2, ..., \beta_I)$ being a vector of parameters and c_β a normalization coefficient; see [8] and references therein. From observed data in the form of a collection of graphs, there are significant challenges to estimate the parameters β. In [8], we find an approach that relies on graph limits in the sense of Lovász and large-deviation results for random graphs, and leads to an infinite-dimensional problem whose optimal value is an estimate of the crucial normalization constant c_β.

Specifically, following [8], we define

$$\begin{aligned}
\psi_0(f) &= \int_0^1 \int_0^1 \tfrac{1}{2} f(x_1, x_2) \log f(x_1, x_2) + \tfrac{1}{2}(1 - f(x_1, x_2)) \log(1 - f(x_1, x_2)) dx_1 dx_2 \\
\psi_1(f) &= \int_0^1 \int_0^1 f(x_1, x_2) dx_1 dx_2 \\
\psi_2(f) &= \int_0^1 \int_0^1 \int_0^1 f(x_1, x_2) f(x_2, x_3) f(x_1, x_3) dx_1 dx_2 dx_3.
\end{aligned}$$

The infinite-dimensional problem is then to

$$\text{minimize } \psi_0(f) - \beta_1 \psi_1(f) - \beta_2 \psi_2(f) \text{ such that } f \text{ symmetric and } 0 \le f \le 1$$

over all measurable functions on $[0, 1]^2$. Here, symmetric means that $f(x_1, x_2) = f(x_2, x_1)$ for all $(x_1, x_2) \in [0, 1]^2$. An approach relying on epi-splines for solving this problem is currently under investigation. Figure 5 provides an example of a minimizing function f for the choice $\beta_1 = 4$ and $\beta_2 = -7$. This problem only indirectly relates to "fitting data," and shows the breath of possible applications of the epi-spline technology.

3 Problem Formulations

As indicated above, FIP is an optimization problem and we now turn to its formulation. In particular, we make distinction between a "true," conceptual problem and an approximate problem to be solved computationally. The section ends with formulation of constraints derived from external information.

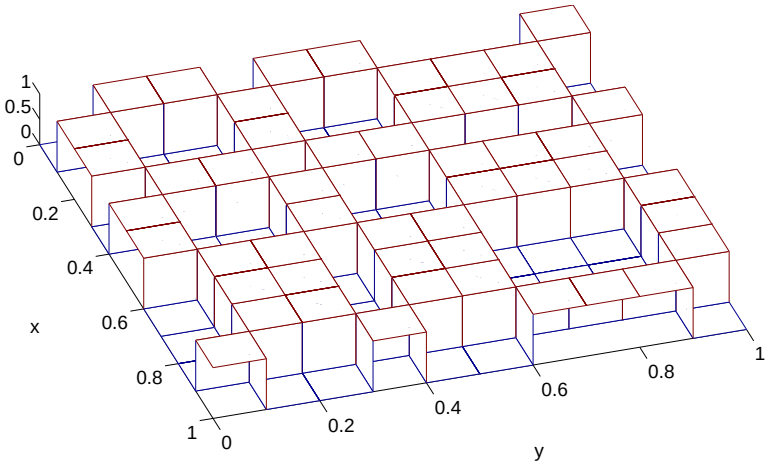

Figure 5: Example of minimizing function f in graph density problem.

3.1 True Problem

We formulate FIP as the problem to determine a function f defined on $\mathbb{R}^n$ that minimizes some criterion given by a functional ψ, while also satisfying constraints given by a feasible set F. The problem may be conceptual, involving information not available and requiring operations not implementable during its solution. This "true problem" therefore takes the form

$$\text{True Problem} \quad (P): \qquad \min \psi(f) \text{ such that } f \in F \subseteq \mathcal{F},$$

where $\mathcal{F}$ is a space of functions. The criterion functional ψ could be, for example,

$$\psi(f) = \sum_{j=1}^{J} (y^j - f(x^j))^2$$
$$\psi(f) = \sum_{j=1}^{J} |y^j - f(x^j)|$$
$$\psi(f) = \max_{j=1,\ldots,J} |y^j - f(x^j)|$$

where $\{(x^j, y^j)\}_{j=1}^J$ is observed data. These terms express errors from the observed data as measured by mean squared, mean absolute, and max absolute errors, respectively. More generally for a known reference function f^0, we may have

$$\psi(f) = \|f - f^0\|,$$

where $\|\cdot\|$ is a norm defined on the space of functions under consideration. For random variables X and Y, with X n-dimensional, expressing possible "future" data, examples of criteria are

$$\begin{aligned}
\psi(f) &= E[f(X)] \\
\psi(f) &= E[\max\{0, Y - f(X)\}]/(1-\alpha) + E[Y - f(X)] \\
\psi(f) &= \mathcal{E}(Y - f(X)).
\end{aligned}$$

The first example focuses on the expected value of the random variable $f(X)$ as arises in density estimation using log-likelihood maximization and an exponential transformation; see [21]. The second expression states the Koenker-Bassett error used in quantile regression, with $\alpha \in [0, 1)$. The third gives the error between random variables Y and $f(X)$ as expressed by an error measure, of which the Koenker-Bassett and mean squared errors are special cases; see [17] for other examples that lead to many different types of generalized regression. Two additional examples are furnished by

$$\begin{aligned}
\psi(f) &= \int \|f''(x)\|^2 dx \\
\psi(f) &= \min_x f(x),
\end{aligned}$$

which do not directly relate to the data. The first one is common in applications such as interpolation. Here the criterion is to obtain a function with minimum "variation" as measured by the integrated squared-value of the second-order derivative or more generally a squared norm of the Hessian matrix. The last example illustrates the versatility of the framework as it allows for criteria functionals that themselves involve optimization.

The feasible region F likewise comes in a large variety of forms. The restrictions to functions that are smooth, convex, monotone, log-concave[2] naturally arise in applications. For example, an analyst may be rather certain that increasing input results in increasing output in a regression analysis. Consequently, she should restrict the consideration to increasing functions. The prevalence of "normal-looking" probability density functions in an area may convince an analyst to only consider log-concave densities, which have only one mode. However, the possibilities extend much further. The functions of interest in an application may be known to attain specific values at a finite number of points, or be zero, $-\infty$, or ∞ outside a certain (compact) set. The functions could be nonsmooth, but with subgradients that are contained in certain sets and possess specific properties, or could be within some distance from a reference function. In fact, any one application may need to contend with many or all of this external information at the same time. At the end of this section, we give some concrete examples of how these pieces of information can be formulated mathematically within an epi-spline framework.

The distinction between a criterion functional and constraints defining the feasible set is less important than it first appears. It is well-known in practical application of optimization models and methods that an objective function can be converted into a constraint and a constraint function can take the place

[2]We recall that a function f is log-concave if $\log f$ is concave.

as objective function with computational and modeling benefits. However, some requirements such as continuity, convexity, and differentiability are most naturally formulated as constraints. Quantifications of "goodness-of-fit" lend themselves as criteria functionals. Typically, application specific conditions indicate the most beneficial formulation, with the opportunity to include arbitrary constraints in (P) offering significant flexibility.

Two classical examples provide additional context. A problem of smooth interpolation aims to determine a function f defined on $\mathbb{R}$ that

$$\text{minimizes } \int f''(x)^2 dx \text{ such that } f(x^j) = y^j \text{ for all } j = 1, 2..., J,$$

i.e., to determine the "smoothest" function that interpolates the points (x^j, y^j), $j = 1, 2, ..., J$. When restricted to functions in a certain Sobolev space, the unique solution of this problem is a cubic spline[3] [15]; see also [11, 1] for numerous extensions. The blue line in Figure 2 illustrates such a cubic spline for the data set of Subsection 2.1. Cubic smoothing splines balance interpolation of the data with "smoothness" of the curve and arise as optimal solutions of

$$\min \sum_{j=1}^{J} (y^j - f(x^j))^2 + \lambda \int f''(x)^2 dx,$$

where $\lambda \geq 0$ is a smoothing penalty [26, 12]. The black dashed line of Figure 2 provides an illustration for $\lambda = 1 \cdot 10^{-4}$. Other "regularizations" by ℓ_1- and ℓ_0-norms lead to similar problems. It is clear that these examples are special cases of the true problem (P).

In the interpolation and smoothing spline examples, optimal solutions are automatically cubic splines and the choice of function space to consider falls naturally to a Sobolev space to ensure existence and integrability of second-order derivatives. The general case (P) requires more care to ensure a sufficiently rich class of functions that can capture (essentially) all possibilities arising in practice. We would like to allow for discontinuous functions, functions with arbitrary rates of growth, for example unbounded derivatives, and functions that take on the values $-\infty$ and ∞. Discontinuities certainly arise in the nonparametric estimation of densities, in response surface building, and in curve fitting. Curve fitting may also lead to functions that grow too fast to be integrable in some sense. The possibility of function values $-\infty$ and ∞ may be needed when implicit constraints are present, for example in curve fitting of functions with effective domain less than the whole domain; it may also arise in applications involving rescaling, exponential rescaling for instance, where zero values needs to be allowed. Consequently, we let the space of function under consideration, $\mathcal{F}$, be the set, or possibly a subset, of lower semi-continuous (lsc) functions from $\mathbb{R}^n$ to the extended real line $\overline{\mathbb{R}} := \mathbb{R} \cup \{-\infty, \infty\}$, excluding the trivial function $f \equiv \infty$, which is identical to infinity everywhere. The left portion of Figure 6 illustrates a lsc function on $\mathbb{R}$. As shown, a lsc function may be *extended real-valued* with values $-\infty$ and ∞, and

[3] Cubic splines are piecewise polynomial functions of third degree that are twice continuously differentiable.

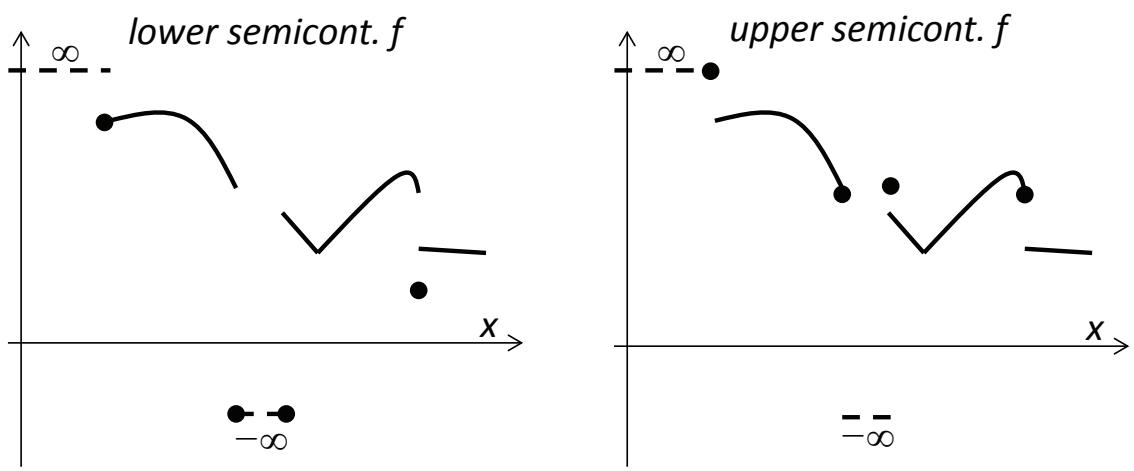

Figure 6: Lower (left) and upper (right) semi-continuous functions.

have discontinuities at which point the function "jumps down." The formal definition of a lsc function requires additional notation. For any f on $\mathbb{R}^n$, we let

$$\liminf_{x' \to x} f(x') := \lim_{\delta \downarrow 0} \left[\inf_{x' \in \mathbb{B}(x,\delta)} f(x') \right],$$

where $\mathbb{B}(x, \delta) := \{x' \in \mathbb{R}^n \mid \|x' - x\| \leq \delta\}$ is the ball of radius δ centered at x. Informally, we think of $\liminf_{x' \to x} f(x')$ as the smallest value of f "near" x. Then,

$$\text{a function } f \text{ is lsc at a point } x \text{ if } \liminf_{x' \to x} f(x') \geq f(x).$$

A function is lsc if it is lsc for all $x \in \mathbb{R}^n$. We denote by lsc-fcns($\mathbb{R}^n$) this set of lsc functions, excluding $f \equiv \infty$. The lsc functions are complemented by upper semi-continuous functions that "jumps up" at points of discontinuity as illustrated by the right portion of Figure 6. The definition is similar. In fact, the lsc functions yield the upper semi-continuous functions after a sign change. A parallel development with such functions is therefore mostly superfluous.

Since external information may indicate that the consideration of, for example, continuous or continuously differentiable functions suffices, not all applications require the full generality of lsc-fcns($\mathbb{R}^n$). We therefore let $\mathcal{F}$ in the true problem be equal to lsc-fcns($\mathbb{R}^n$) or an appropriate subset. The choice of representing external information by the constraint set F or alternatively in the definition of the space of functions $\mathcal{F}$ is purely a technicality.

3.2 Approximations

The true problem (P) rarely admits closed form solutions and computational strategies become essential. However, optimization over functions instead of over a finite number of parameters is not

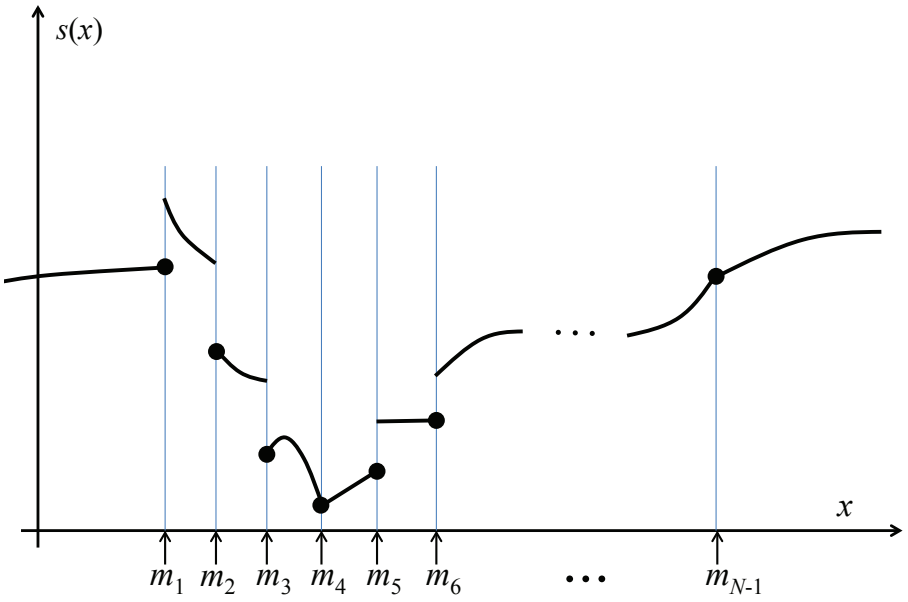

Figure 7: Mesh and epi-spline on $\mathbb{R}$.

implementable in a computational method. The criterion functional may also involve integrals and the number of constraints could be infinite, both requiring some sort of approximation. The true problem could also represent an "ideal" situation with full information that should be contrasted with a problem involving only observed data. Regardless of the situation, there is a need for considering approximations of (P). We start with defining approximations of lsc functions in terms of simpler functions called epi-splines that involve only a finite number of parameters.

Epi-splines are defined on $\mathbb{R}^n$, but we first present the one-dimensional case for simplicity.

One-dimensional epi-splines on a mesh. A *mesh* is a finite number of points

$$-\infty = m_0 < m_1 < m_2 < ..., < m_{N-1} < m_N = \infty$$

on the real line as illustrated by Figure 7. An *epi-spline*[4] of order p on such a mesh is a real-valued function s that

$$\begin{aligned} &\text{on each open interval } (m_{k-1}, m_k),\ k = 1, ..., N, \text{ is polynomial of degree } p \text{ and} \\ &\text{for every } x \in \mathbb{R}, \text{ has } s(x) = \min\left\{\lim_{t\downarrow 0} s(x+t), \lim_{t\downarrow 0} s(x-t)\right\}. \end{aligned}$$

Figure 7 shows an epi-spline of second-order, i.e., $p = 2$, which on each open interval (m_{k-1}, m_k) is a second-degree polynomial. An epi-spline of order $p = 0$ is a piecewise constant function and one of order

[4]In [22] these epi-splines are called lsc epi-splines, but we here exclusively focus on such epi-splines and the prefix is therefore superfluous. Basic epi-splines defined only on a compact interval of $\mathbb{R}$ is given in [20].

$p = 1$ is a piecewise affine function with possibilities of jumps at the mesh-points $m_1, m_2, ..., m_{N-1}$. The second condition ensures that the value $s(x)$ is the smaller of the left and right limits of s at x, which of course exist since s is continuous (polynomial) except at the mesh-points. This ensures that s is lsc.

Epi-splines are structurally related to splines, but are more flexible. In fact, interest in splines of order p with less than the standard $(p-1)$-times continuous differentiability at their "knots" goes back to Curry and Schoenberg [9, 10]. However, mesh-points $m_1, \ldots, m_{N-1}$ should not be identified with the knots of such splines since no assumptions are made about information being available at mesh-points and no continuity requirements are placed on epi-splines at (precisely) these mesh-points. In fact, the partition can be selected completely freely. Continuity and any other condition can still be ensured when needed through constraints in (P) as discussed at the end of this section. Since from an etymological viewpoint the (Greek) prefix "epi" can be interpreted as meaning "higher" or "better," the term epi-splines is certainly appropriate for these more "general" splines. In §4 and §5, we see that the analysis of epi-splines relies heavily on epi-convergence and the epi-topology, which provides further justification for the name.

Higher-dimensional epi-splines. Epi-splines in higher dimensions follow similarly, but require additional notation. We denote by $\operatorname{cl} S$ the closure of a subset S of a Euclidean space. A finite collection $R_1, R_2, ..., R_N$ of open subsets of $\mathbb{R}^n$ is a *partition* of $\mathbb{R}^n$ if

$$\bigcup_{k=1}^{N} \operatorname{cl} R_k = \mathbb{R}^n \text{ and } R_k \cap R_l = \emptyset \text{ for all } k \neq l.$$

There are clearly many possible partitions, but in practice those consisting of rectangular boxes and simplexes appear to suffice. We adopt a "total degree" convention and say that a polynomial in n dimensions is of *total degree* p if it is expressed as a finite sum of polynomial terms each having the sum of the powers of the variables being no larger than p. We note that the total number of terms in such a polynomial is at most $(n+p)!/(n!p!)$. Another connection would have had only minor consequences for the following exposition.

An epi-spline s of order p defined on $\mathbb{R}^n$ with partition $\mathcal{R} = \{R_k\}_{k=1}^N$ is a real-valued function that

$$\begin{aligned} &\text{on each } R_k,\ k = 1, ..., N, \text{ is polynomial of total degree } p \text{ and} \\ &\text{for every } x \in \mathbb{R}^n, \text{ has } s(x) = \liminf_{x' \to x} s(x'). \end{aligned}$$

As in the one-dimensional case, an epi-spline is polynomial on open sets. The second condition ensures that it is also lsc by defining the value at boundary points of the partition appropriately. Figure 8 illustrates an epi-splines of order two on $\mathbb{R}^2$. The partition consists of rectangles. The family of all epi-splines of order p on $\mathbb{R}^n$ with partition $\mathcal{R}$ is denoted by $\text{e-spl}_n^p(\mathcal{R})$. Since an $s \in \text{e-spl}_n^p(\mathcal{R})$, with $\mathcal{R} = \{R_k\}_{k=1}^N$, involves N polynomials of total order p, it is fully characterized by

$$n_e := N(n+p)!/(n!p!) \tag{1}$$

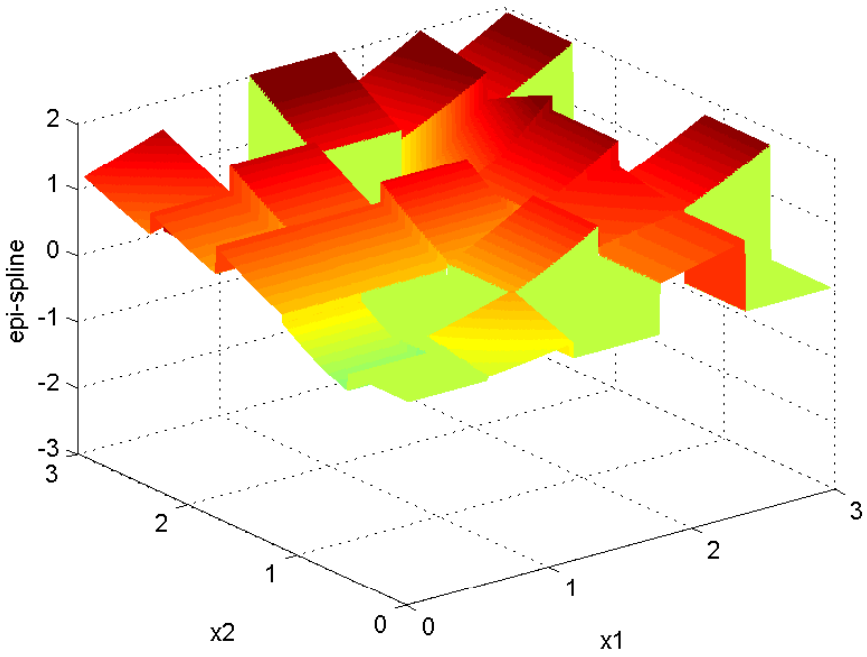

Figure 8: Epi-spline on $\mathbb{R}^2$.

parameters, which may be large but finite.

Approximate problem. To also allow for the possibility of approximations in the criterion functional ψ and the feasible set F, we define an *approximate criterion* ψ^ν and an *approximate feasible set* $F^\nu \subset \mathcal{F}$. Relying on epi-splines, we define the approximate functions under consideration to be

$$\mathcal{S}^\nu \subseteq \text{e-spl}_n^{p^\nu}(\mathcal{R}^\nu) \cap \mathcal{F}.$$

The superscript ν indicates that a family of approximations can be considered, possibly with gradually more refined partition $\mathcal{R}^\nu$, for example. These approximations lead to an

$$\text{Approximate Problem} \quad (P^\nu): \qquad \min \psi^\nu(s) \text{ such that } s \in F^\nu \cap \mathcal{S}^\nu$$

that approximates the true problem (P).

(P^ν) is an optimization over functions, but they are all epi-splines and therefore representable by a finite number of parameters. Consequently, (P^ν) is a *finite-dimensional* optimization problem that is solved by optimizing over the $N^\nu(n+p^\nu)!/(n!p^\nu!)$ (real) parameters describing the family of epi-splines under consideration. Here N^ν is the number of open sets in the partition of $\mathbb{R}^n$. We refer to an optimization problem over such parameters as a *parametric optimization problem* corresponding to (P^ν); see §5 for

further discussion. Under the assumption that additional complications are removed by approximations of the criterion functional and feasible set, the solution of parametric optimization problems can be obtained by standard algorithms, or possibly more efficiently by specialized algorithms in certain cases.

With the introduction of approximations, we need to deal with the possibility that solutions of approximate problems (P^ν) may not relate to those of the true problem (P). Under what conditions will solutions of (P^ν) be approximate solutions of (P)? More fundamentally, can we approximate any lsc function by epi-splines? These questions require the discussion of approximation theory of optimization problems as reviewed in Section 4, with answers provided in Section 5. We end this section, however, with examples of external information and their implementation.

3.3 External Information

External information needs to be converted into mathematical forms and included as constraint in the parametric optimization problem corresponding to (P^ν). The formulation of such constraints depend on the representation of the polynomials in an epi-spline. Of course, there are many possible representations, some of which are known to be numerically more beneficial than others. Here, we only consider one-dimensional epi-splines and the simple representation

$$q^k(x) = a_0^k + a_1^k x + a_2^k x^2 + ... + a_p^k x^p, \quad x \in I\!R, \tag{2}$$

of the polynomial describing an epi-spline on the interval (m_{k-1}, m_k), $k = 1, 2, ..., N$. With N intervals partitioning $I\!R$, the epi-spline is defined by N such polynomials with a total of $N(p+1)$ parameters. We next give some examples of external information and the formulation of corresponding constraints using this representation; see [22] for extensions to higher dimensions and [21] for constraints related to density estimation.

Continuity. An epi-spline is continuous if the polynomials $q^1, q^2, ..., q^N$ defining the epi-spline coincide at the mesh-points m_1, m_2, ..., m_{N-1}. This is easily achieved by the constraints

$$a_0^k + a_1^k m_k + a_2^k m_k^2 + ... + a_p^k m_k^p = a_0^{k+1} + a_1^{k+1} m_k + a_2^{k+1} m_k^2 + ... + a_p^{k+1} m_k^p, \ k = 1, 2, ..., N-1.$$

Of course, this constraint could be enforced only at a subset of the mesh-points to allow for discontinuities in some areas, but not in others as done in Figure 2.

Continuous differentiability. An epi-spline is continuously differentiable if continuous, ensured by the above equations, and the derivatives of the polynomials $q^1, q^2, ..., q^N$ coincide at the mesh-points m_1, m_2, ..., m_{N-1}. This is achieved by the constraints

$$a_1^k + 2a_2^k m_k + ... + pa_p^k m_k^{p-1} = a_1^{k+1} + 2a_2^{k+1} m_k + ... + pa_p^{k+1} m_k^{p-1}, \ k = 1, 2, ..., N-1,$$

where we assume that $p \geq 1$. Continuous differentiability is automatic for a continuous epi-spline of order $p = 0$.

Fixed values. We ensure that an epi-spline satisfies the function value $s(x)$ on a set $S_k \subset (m_{k-1}, m_k)$ by the constraints

$$a_0^k + a_1^k x + a_2^k x^2 + ... + a_p^k x^p = s(x),\ x \in S_k.$$

This may at first give the impression that an infinite number of constraints is needed. However, if S_k has more than $p+1$ distinct points, then it suffices to select $p+1$ distinct points at which to enforce the constraints as a polynomial of degree p is uniquely defined by its value at $p+1$ points. The equality can naturally be replaced by inequality if only bounds are available. Moreover, if the values of an epi-spline is of no interest beyond a certain mesh-point, then the polynomials defining the epi-spline beyond that point is of course immaterial and can be ignored.

Monotonicity. We ensure that an epi-spline of order $p \geq 1$ is nonincreasing by the constraints

$$a_1^k + 2a_2^k x + ... + pa_p^k x^{p-1} \leq 0,\ x \in (m_{k-1}, m_k), k = 1, 2, ..., N, \text{ and}$$
$$a_0^k + a_1^k m_k + a_2^k m_k^2 + ... + a_p^k m_k^p \geq a_0^{k+1} + a_1^{k+1} m_k + a_2^{k+1} m_k^2 + ... + a_p^{k+1} m_k^p,\ k = 1, 2, ..., N-1.$$

The first set of constraints ensures that the polynomials making up an epi-spline are nonincreasing on the intervals on which they define the epi-spline. The second set imposes the restriction that when moving from left to right, the epi-spline must not jump up at mesh-points. The second requirement is automatically satisfied for continuous epi-splines. In the case of $p = 2$, the first condition simplifies to the two constraints

$$a_1^k + 2a_2^k m_{k-1} \leq 0 \text{ and } a_1^k + 2a_2^k m_k \leq 0$$

as in that case the derivative of the epi-spline is simply linear. For any p, the first *and* the second conditions hold if

$$a_1^k + 2a_2^k m_k + ... + pa_p^k m_k^{p-1} \leq 0$$

under the additional assumption that the epi-spline is convex since then the epi-spline is continuous with an nondecreasing (left/right-sided) derivative.

Convexity. We ensure that an epi-spline is convex by the continuity constraints above and

$$2a_2^k + ... + p(p-1)a_p^k x^{p-2} \geq 0,\ x \in (m_{k-1}, m_k), k = 1, 2, ..., N, \text{ and}$$
$$a_1^k m_k + 2a_2^k m_k + ... + pa_p^k m_k^{p-1} \leq a_1^{k+1} m_k + 2a_2^{k+1} m_k + ... + pa_p^{k+1} m_k^{p-1},\ k = 1, 2, ..., N-1.$$

The first set of constraints ensures that the second-order derivative of the polynomials making up an epi-spline are nonnegative and therefore convex on the intervals on which they define the epi-spline. For $p < 2$, the constraints are superfluous. The second set imposes the restriction that when moving from left to right, the derivative of the epi-spline must not jump down at mesh-points. The second requirement is automatically satisfied for continuous differentiable epi-splines and can be ignored for the case $p = 0$. If an epi-spline is of second order, then the first set of constraints simplifies to $a_2^k \geq 0$ for $k = 1, ..., N$. If $p = 3$, the first set of constraints simplifies to

$$2a_2^k + 6a_3^k m_{k-1} \geq 0 \text{ and } 2a_2^k + 6a_3^k m_k \geq 0$$

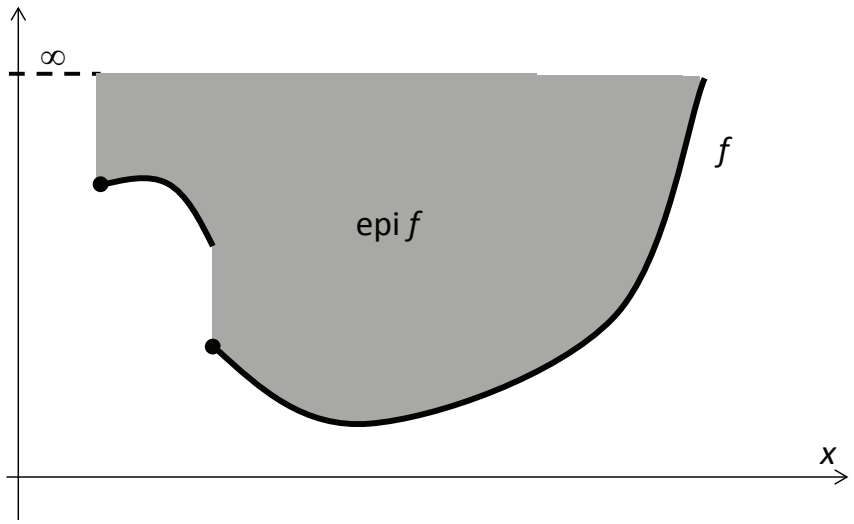

Figure 9: Epi-graph of a function f on $\mathbb{R}$.

because then the second-order derivative is simply linear.

We note that the above constraints, and many similar one, are *linear* in the parameters describing an epi-spline. Consequently, their addition in a parametric optimization problem corresponding to (P^ν) requires little additional computational effort.

4 Background

The examination of epi-splines and the relationship between the true problem (P) and approximate problems (P^ν) rely on variational analysis and, especially, the approximation theory of optimization problems with the notion of epi-convergence taking center stage. We here provide the essential components; see [18, 4] for a comprehensive treatment.

We view a function on $\mathbb{R}^n$ through its *epi-graph*

$$\text{epi}\, f := \{(x, x_0) \in \mathbb{R}^{n+1} \mid f(x) \leq x_0\},$$

i.e., the set of points in $\mathbb{R}^{n+1}$ that lies no lower than the graph of f as illustrated in Figure 9. We note that

$$f \in \text{lsc-fcns}(\mathbb{R}^n) \text{ if and only if } \text{epi}\, f \text{ is a nonemptly closed subset of } \mathbb{R}^{n+1}.$$

Distances between such functions can therefore be based on distances between (closed) sets in $\mathbb{R}^{n+1}$.

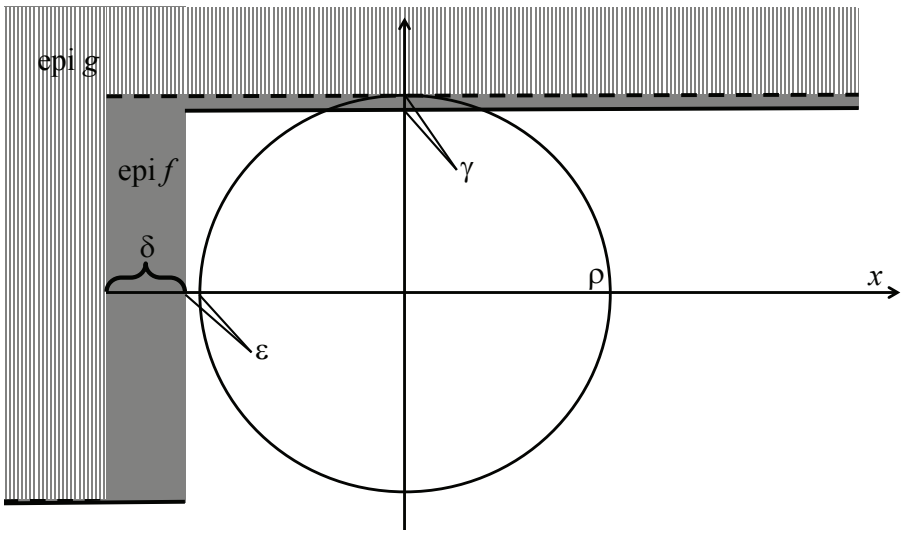

Figure 10: Illustration of distances: $d\!\!l_\rho(f,g) = \delta$ and $\hat{d\!\!l}_\rho(f,g) = \gamma$.

We start with notation and let $\rho I\!B = I\!B(0,\rho)$ be the closed call in a Euclidean space centered at the origin with radius $\rho \geq 0$ and

$$d(y,S) := \inf_{y' \in S} \|y - y'\|$$

be the standard distance between a point y and a subset S of a Euclidean space. We use the notation $A + B = \{a + b \mid a \in A, b \in B\}$ for the Minkowski sum of two sets A and B in a Euclidean space.

The classical Pompeiu-Hausdorff distance between sets $C, D \subset I\!R^n$,

$$d\!\!l_\infty(C,D) := \sup_{y \in I\!R^n} |d(y,C) - d(y,C)| = \inf\{\eta \geq 0 \mid C \subset D + \eta I\!B, D \subset C + \eta I\!B\}$$

is not useful in the present context as epi-graphs are unbounded sets and this distance is easily infinity. We therefore turn to two distances that depart from the Pompeiu-Hausdorff distance in different directions (see [2] and [18, §4.H]).

Focusing now on epi-graphs, we first define the *ρ-epi-distance* between two functions f and g on $I\!R^n$, which is given by a restrictions of the first formula for the Pompeiu-Hausdorff distance:

$$d\!\!l_\rho(f,g) = \sup_{\bar{x} \in \rho I\!B} |d(\bar{x}, \operatorname{epi} f) - d(\bar{x}, \operatorname{epi} g)|, \quad \rho \geq 0.$$

Obviously, $d\!\!l_\rho(f,g) = d\!\!l_\infty(\operatorname{epi} f, \operatorname{epi} g)$ for $\rho = \infty$. As illustrated in Figure 10, $d\!\!l_\rho(f,g)$ gives the largest difference in distance between a point $\bar{x} \in \rho I\!B$ and the respective epi-graphs. In this figure, with $f(x) = \rho - \gamma$ for $x > -\rho - \varepsilon$ and $f(x) = -\rho$ for $x \leq -\rho - \varepsilon$; $g(x) = \rho$ for $x > -\rho - \delta - \varepsilon$ and $g(x) = -\rho$ for $x \leq -\rho - \delta - \varepsilon$; and $\delta + \varepsilon < \rho$ and ε, γ small, the point $\bar{x} = (-\rho, 0)$ provides the maximizing point,

with $d(\bar{x}, \operatorname{epi} f) = \varepsilon$ and $d(\bar{x}, \operatorname{epi} g) = \delta + \varepsilon$. Consequently, $\mathbb{d}_\rho(f, g) = \delta$.

The second distance, the *ρ-epi-distance estimate*, relies on the second formula for the Pompeiu-Hausdorff distance, but limits the focus to the ball centered at the origin with radius ρ:

$$\hat{\mathbb{d}}_\rho(f, g) = \inf\{\eta \geq 0 \mid \operatorname{epi} f \cap \rho\mathbb{B} \subset \operatorname{epi} g + \eta\mathbb{B}, \operatorname{epi} g \cap \rho\mathbb{B} \subset \operatorname{epi} f + \eta\mathbb{B}\}, \quad \rho \geq 0.$$

Again, $\hat{\mathbb{d}}_\rho(f, g) = \mathbb{d}_\infty(\operatorname{epi} f, \operatorname{epi} g)$ for $\rho = \infty$. Figure 10 illustrates $\hat{\mathbb{d}}_\rho$, which involves "padding" the first epi-graph so that it includes the second one, and vice versa. In this figure, $\operatorname{epi} g \cap \rho\mathbb{B}$ contains the single point $(0, \rho)$ which is clearly contained in $\operatorname{epi} f$ and $\operatorname{epi} g$ only needs to be padded with γ to ensure that $\operatorname{epi} f \cap \rho\mathbb{B} \subset \operatorname{epi} g + \gamma\mathbb{B}$. Consequently, $\hat{\mathbb{d}}_\rho(f, g) = \gamma$.

Neither $\mathbb{d}_\rho$ nor $\hat{\mathbb{d}}_\rho$ is a metric on lsc-fcns($\mathbb{R}^n$). The ρ-epi-distance $\mathbb{d}_\rho$ is a pseudo-metric, but $\hat{\mathbb{d}}_\rho$ is not. Obviously, if $\rho\mathbb{B}$ is "small," then $\mathbb{d}_\rho(f, g)$ may very well be zero without f and g being equal. It is apparent that all values of ρ need to come into play. This is accomplished in the *epi-distance*

$$\mathbb{d}(f, g) := \int_0^\infty \mathbb{d}_\rho(f, g) e^{-\rho} d\rho,$$

which then leads to the following fact:

$$\mathbb{d} \text{ is a metric on the space lsc-fcns}(\mathbb{R}^n).$$

We say that functions $f^\nu \in \text{lsc-fcns}(\mathbb{R}^n)$ *epi-converges* to a function $f \in \text{lsc-fcns}(\mathbb{R}^n)$ if $\mathbb{d}(f^\nu, f) \to 0$. Epi-convergence is also characterized by $\mathbb{d}_\rho$ and $\hat{\mathbb{d}}_\rho$:

For functions $f^\nu, f \in \text{lsc-fcns}(\mathbb{R}^n)$ and $\hat{\rho} \geq 0$, the following is equivalent:

$$\begin{aligned} &\mathbb{d}(f^\nu, f) \to 0 \\ &\mathbb{d}_\rho(f^\nu, f) \to 0 \text{ for } \rho \geq \hat{\rho} \\ &\hat{\mathbb{d}}_\rho(f^\nu, f) \to 0 \text{ for } \rho \geq \hat{\rho}. \end{aligned}$$

The epi-distance induces the *epi-topology* (in topology circles referred to as the Attouch-Wets topology) on lsc-fcns($\mathbb{R}^n$). In fact, by Theorem 7.58 of [18], $(\text{lsc-fcns}_{\not\equiv\infty}(\mathbb{R}^n), \mathbb{d})$ is a complete metric space. It is also separable and therefore a Polish space, with in fact epi-splines given in terms of polynomials with rational coefficients furnishing a countable dense subset [22]. However, lsc-fcns($\mathbb{R}^n$) is not a vector space[5] as $-f \notin \text{lsc-fcns}(\mathbb{R}^n)$ for $f \in \text{lsc-fcns}(\mathbb{R}^n)$ given by $f(x) = 0$ if $x \in [0, \infty)^n$ and $f(x) = 1$ otherwise. We note however that it is a cone, i.e., $\lambda f \in \text{lsc-fcns}(\mathbb{R}^n)$ for $\lambda \geq 0$ and $f \in \text{lsc-fcns}(\mathbb{R}^n)$ and also convex if the point $\{\infty\}$ (i.e., the function that is infinity everywhere) is included.

[5] We define addition of functions and multiplication with a scalar in the usual "pointwise" manner. To handle extended real-values, we adopt the conventions that $\infty + a = \infty$ and $-\infty + a = -\infty$ for $a \in \mathbb{R}$, $\infty + \infty = \infty + (-\infty) = -\infty + \infty = \infty$, $\lambda \cdot \infty = -\infty$ for $\lambda < 0$, $0 \cdot \infty = 0$, and $\lambda \cdot \infty = \infty$ for $\lambda > 0$, and similarly for $\lambda \cdot (-\infty)$.

A parallel, slightly more general, development focusing on nonempty closed set in $\mathbb{R}^n$, instead of epi-graphs of lsc functions, is also possible and leads to *set convergence* in the sense of Painlevé-Kuratowski. Such convergence is characterized by $\mathbb{d}$, $\mathbb{d}_\rho$, and $\hat{\mathbb{d}}_\rho$, similar to the above characterization of epi-convergence, with the slight change in definition of these distances consisting of replacing epi-graphs by closed sets; see [18, Chapter 4] and [6] for further details about topologies on closed sets.

Connections between the various distance are provided by [18, Exercise 7.60]. For example, for functions f, g on $\mathbb{R}^n$ not identical to ∞,

(i) $\hat{\mathbb{d}}_\rho(f,g) \le \mathbb{d}_\rho(f,g) \le \hat{\mathbb{d}}_{\rho'}(f,g)$, when $\rho' \ge 2\rho + \max\{d(0, \operatorname{epi} f), d(0, \operatorname{epi} g)\}$

(ii) $\mathbb{d}(f,g) \ge (1-e^{-\rho})|d(0, \operatorname{epi} f) - d(0, \operatorname{epi} g)| + e^{-\rho}\mathbb{d}_\rho(f,g)$

(iii) $\mathbb{d}(f,g) \le (1-e^{-\rho})\mathbb{d}_\rho(f,g) + e^{-\rho}(\max\{d(0, \operatorname{epi} f, d(0, \operatorname{epi} g)\} + \rho + 1)$

(iv) $\mathbb{d}_\rho(f,g) = \hat{\mathbb{d}}_\rho(f,g)$ for any $\rho \ge 0$ if f, g convex with $f(0) \le 0$ and $g(0) \le 0$.

As is clear from these results, the distances are tied to the origin of $\mathbb{R}^{n+1}$. Although formulae for other "anchor" points are also possible, the simplest way of utilizing these estimates is to translate the functions f and g favorably. Item (iv) highlights the possibilities in that direction in the case of convex functions.

It is apparent that

$$\mathbb{d}_\rho(f,g) \le \|f-g\|_\infty := \sup_{x \in \mathbb{R}^n} |f(x) - g(x)|$$

and since $\int_0^\infty e^{-\rho} d\rho = 1$, that also

$$\mathbb{d}(f,g) \le \|f-g\|_\infty.$$

Of course, with the possibilities of the function values $-\infty$ and ∞, the right-hand sides may easily be ∞ making reliance on $\|\cdot\|_\infty$ impractical. Even for finite-valued functions, it is clear that convergence in the epi-distance does not imply convergence in $\|\cdot\|_\infty$ as the following simple example shows. Suppose that $f^\nu(x) = 0$ if $x \le 0$ and $f^\nu(x) = x/\nu$ otherwise. We also define $f^0(x) = 0$ for all $x \in \mathbb{R}$; see Figure 11. Clearly, $\|f^\nu - f^0\|_\infty = \infty$ for all ν. However, for any $\rho \ge 0$, $\mathbb{d}_\rho(f^\nu, f^0) \le \rho/\nu$ and therefore $\mathbb{d}(f^\nu, f^0) \le (1/\nu)\int_0^\infty \rho e^{-\rho} d\rho = 1/\nu$. Consequently, $\mathbb{d}(f^\nu, f^0) \to 0$, but $\|f^\nu - f^0\|_\infty \not\to 0$.

Pointwise convergence of a sequence of functions is also not equivalent to epi-convergence even if both pointwise and epigraphical limits exist as the following simple example shows. Suppose that $f^\nu(x) = 0$ if $x = 1/\nu$ and $f^\nu(x) = 1$ otherwise. Clearly, the pointwise limit of f^ν, i.e., the function defined by $\lim_\nu f^\nu(x)$ for every x, is the function that is unity everywhere. In contrast, f^ν epi-converges to the function f^0 with $f^0(x) = 0$ for $x = 0$ and $f^0(x) = 1$ otherwise, i.e., $\mathbb{d}(f^\nu, f^0) \to 0$. In fact, $\mathbb{d}_\rho(f^\nu, f^0) = \hat{\mathbb{d}}_\rho(f^\nu, f^0) = 1/\nu$; see Figure 12.

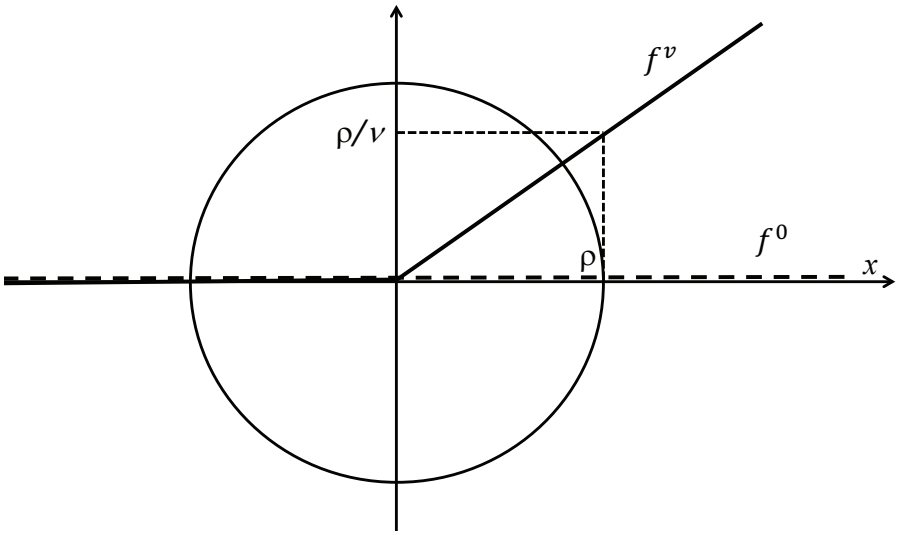

Figure 11: Illustration of epi-convergence without uniform convergence.

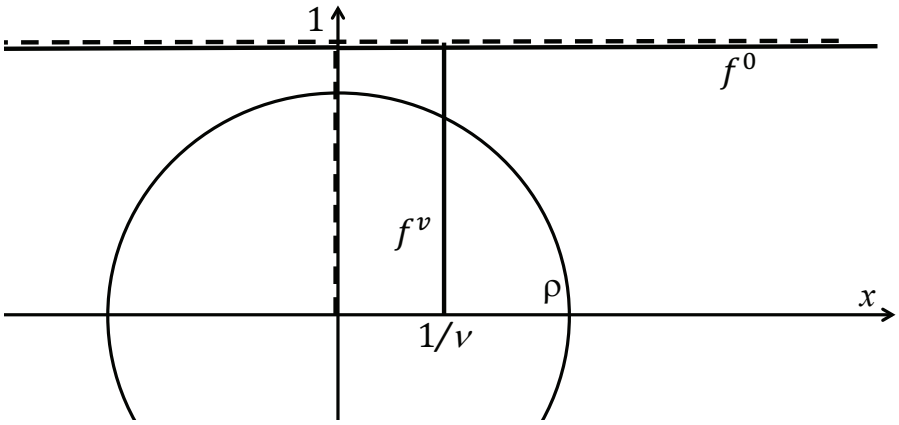

Figure 12: Illustration of epi-convergence and pointwise convergence.

Specific estimates for epi-splines are provided in [22]: For $s, s' \in \text{e-spl}_n^p(\mathcal{R})$, with $\mathcal{R} = \{R_k\}_{k=1}^N$, one has for any $\rho \geq 0$,

$$\text{(i) } d\!\!\!l(s, s') \leq \max_{k=1,\ldots,N} \sup_{x \in R_k} |s(x) - s'(x)|$$
$$\text{(ii) } d\!\!\!l_\rho(s, s') \leq \max_{k=1,\ldots,N} \sup_{x \in R_k} |s(x) - s'(x)|$$
$$\text{(iii) } \hat{d\!\!\!l}_\rho(s, s') \leq \max_{k=1,\ldots,N} \hat{d\!\!\!l}_\rho(s_k, s'_k).$$

These results provide a quantification of epi-convergence of functions in lsc-fcns($\mathbb{R}^n$). However, we need to go one step further and define epi-convergence of *optimization problems* defined over such functions.

We next provide a definition of epi-convergence of the approximate problems (P^ν) to the true problem (P). In view of the above results, these are problems defined on the metric space (lsc-fcns($\mathbb{R}^n$), $d\!\!\!l$) and we therefore follow [3]:

A sequence $\{(P^\nu)\}_{\nu \in \mathbb{N}}$ epi-converges to (P) if

(i) for every sequence $\{s^\nu\}_{\nu \in K}$, with K an infinite subsequence of the positive integers, $s^\nu \in F^\nu \cap \mathcal{S}^\nu$, and $d\!\!\!l(s^\nu, f) \to 0$, we have that $f \in F$ and $\liminf_\nu \psi^\nu(s^\nu) \geq \psi(f)$;

(ii) for every $f \in F$, there exists a sequence $\{s^\nu\}_{\nu=1}^\infty$, with $s^\nu \in F^\nu \cap \mathcal{S}^\nu$, such that $d\!\!\!l(s^\nu, f) \to 0$ and $\limsup_\nu \psi^\nu(s^\nu) \leq \psi(f)$.

The main consequence of epi-convergence in this context is the fact that it implies that solutions of the approximate problems tend to those of the true problem. Let V and V^ν be the minimum values of (P) and (P^ν), respectively. Specifically, by [3, Theorem 2.5],

> if (P^ν) epi-converges to (P), s^k minimizes (P^{ν_k}), and $d\!\!\!l(s^k, f) \to 0$, then f is a minimizer of (P) and $\lim_k V^{\nu_k} = V$.

This result therefore provides a direct path to an answer to the earlier question whether a solution of an approximate problem (P^ν) would be an approximate solution of (P): one needs to ensure epi-convergence of (P^ν) to (P).

5 Theory

A series of results are available about the relationship between (P^ν) to (P) and their solutions as well as between epi-splines and lsc functions. Results in the context of probability density estimation are established in [21], for other cases with one-dimensional functions see [20], and more generally we refer to [22]. Here we give three central results dealing with epi-convergence of (P^ν) to (P), the rate of convergence of corresponding solutions, and the ability of epi-splines to approximate to an arbitrary

level of accuracy any lsc function.

Epi-convergence. A sufficient condition for epi-convergence of (P^ν) to the true problem (P) relies on continuous convergence of the approximate criterion ψ^ν to the true criterion ψ. Often, ψ^ν is simply identical to ψ for all ν. For the general case, we recall that ψ^ν converges continuously to ψ relative to $\mathcal{F}$ if for every $f \in \mathcal{F}$ and sequence $\{s^\nu\}_{\nu=1}^\infty$, with $s^\nu \in \mathcal{F}$ and $d\!l(s^\nu, f) \to 0$, $\psi^\nu(s^\nu) \to \psi(f)$. We use the notation $\operatorname{int} F$ to denote the interior of $F \subset \mathcal{F}$ (with respect to the epi-topology). We establish in [22] that if

(i) ψ^ν converges continuously to ψ relative to $\mathcal{F}$

(ii) $\cup_{\nu=1}^\infty \mathcal{S}^\nu$ is dense in $\mathcal{F}$

(iii) F^ν set-converge to $F = \operatorname{cl}(\operatorname{int} F)$,

then (P^ν) epi-converges to (P).

The first sufficient condition implies that ψ is continuous with respect to the epi-topology. The second condition relates to the ability of epi-splines to approximate arbitrary lsc functions, which we deal with in the next paragraph. The last part of the third condition is a constraint qualification that avoids "isolated" feasible points that cannot easily be approximated. Numerous simplification occurs if $\mathcal{F} \subset \text{e-spl}_n^p(\mathcal{R})$ for some partition $\mathcal{R}$ and order p, which implies that both (P^ν) to (P) are finite-dimensional, as discussed at the end of the section.

Approximation by epi-splines. To allow for approximation of arbitrary lsc function, we consider a sequence of partitions that are gradually refined. Specifically, we say that a sequence $\{\mathcal{R}^\nu\}_{\nu=1}^\infty$ of partitions of $I\!R^n$, with $\mathcal{R}^\nu = \{R_k^\nu\}_{k=1}^{N^\nu}$, is an *infinite refinement* if

> for every $x \in I\!R^n$ and $\varepsilon > 0$, there exists a positive integer $\bar\nu$ such that
> $R_k^\nu \subset I\!B(x, \varepsilon)$ for every $\nu \geq \bar\nu$ and k satisfying $x \in \operatorname{cl} R_k^\nu$.

A simple example of an infinite refinement on $I\!R$ is to take $N^\nu = 2\nu + 2$, $R_1^\nu = (-\infty, -\sqrt{\nu})$, $R_k^\nu = ((k-\nu-2)/\sqrt{\nu}, (k-\nu-1)/\sqrt{\nu})$ for $k = 2, 3, ..., 2\nu+1$, and $R_{2\nu+2}^\nu = (\sqrt{\nu}, \infty)$. Then $\bar\nu > \max\{x^2, \varepsilon^{-2}\}$ satisfies the above condition. Obviously, much flexibility exists in constructing such infinite refinements.

A main result in [22] is then that

> for any nonnegative integer p and $\{\mathcal{R}^\nu\}_{\nu=1}^\infty$ an infinite refinement on $I\!R^n$,
>
> $$\bigcup_{\nu=1}^\infty \text{e-spl}_n^p(\mathcal{R}^\nu) \text{ is dense under the epi-topology in } \text{lsc-fcns}(I\!R^n).$$

Consequently, epi-splines, even those of order zero, can approximate to an arbitrary level of accuracy any lsc function. The optimization over epi-splines in (P^ν) is therefore justified.

Rate of convergence. Solutions of (P^ν) tend to those of (P) at rates that depends on several factors and a full analysis along the lines of [5] and references therein is beyond the scope of this tutorial. We here consider the case when $\mathcal{F} \subset \text{e-spl}_n^p(\mathcal{R})$ for some partition $\mathcal{R} = \{R_k\}_{k=1}^N$ and order p, i.e., the true problem (P) is finite dimensional. Of course, in view of the flexibility of epi-splines, there may be little too loose from a practical perspective to adopt this simplification from the outset. In view of the finite number of parameters describing an epi-spline, (P) corresponds then to a parametric optimization problem

$$\text{Parametric True Problem} \quad (\bar{P}): \qquad \min \bar{\psi}(r) \text{ such that } r \in R \subset \mathbb{R}^{n_e},$$

where R is a feasible region corresponding to the constraint set F, $\bar{\psi}$ is a criterion function expressed as a function of the parameters r, and n_e is defined in (1). If every $s \in \text{e-spl}_n^p(\mathcal{R})$ is of the form $s = \langle c(\cdot), r\rangle$, with $r \in \mathbb{R}^{n_e}$ and $c = (c_1, c_2, ..., c_{n_e})$ a set of basis functions[6] for the corresponding polynomials, then $\bar{\psi}(r) = \psi(\langle c(\cdot), r\rangle)$ and $R = \{r \in \mathbb{R}^{n_e} \mid \langle c(\cdot), r\rangle \in F\}$.

Similarly, a parametric optimization problem corresponding to (P^ν) takes the form

$$\text{Parametric Approximate Problem} \quad (\bar{P}^\nu): \qquad \min \bar{\psi}^\nu(r) \text{ such that } r \in R^\nu,$$

where $R^\nu = \{r \in \mathbb{R}^{n_e} \mid \langle c(\cdot), r\rangle \in F^\nu \cap \mathcal{S}^\nu\}$ and $\bar{\psi}^\nu(r) = \psi^\nu(\langle c(\cdot), r\rangle)$. We quantify next the relationship between solutions of $(\bar{P}^\nu)$ and $(\bar{P})$.

We focus here on *near-optimal* solutions of $(\bar{P}^\nu)$ that are indeed the solutions provided by numerical solvers. A benefit of such an approach is that we avoid quantifying the "conditioning" of the problems near optimal solutions; see [18, Section 7.J] for results in that direction. We therefore define the ε-optimal solutions for $(\bar{P}^\nu)$, which for $\varepsilon \geq 0$, is given by

$$\bar{R}_\varepsilon^\nu = \{r \in R^\nu \mid \bar{\psi}^\nu(r) \leq \bar{V}^\nu + \varepsilon\},$$

with $\bar{V}^\nu$ being the optimal value of $(\bar{P}^\nu)$. We also say that a function φ is Lipschitz on $\rho\mathbb{B}$ with constant κ if

$$|\varphi(r) - \varphi(r')| \leq \kappa \|r - r'\| \text{ for all } r, r' \in \rho\mathbb{B}.$$

A quantitative approximation result can then be deduced from Theorem 7.69 and Example 7.62 in [18]:

> Suppose that $\bar{\psi}, \bar{\psi}^\nu$ are finite convex functions, R, R^ν are closed convex sets, and $\rho_0 \in (0, \infty)$ is such that there exists $r, r^\nu \in \rho_0\mathbb{B}$ optimal in $(\bar{P})$ and $(\bar{P}^\nu)$, respectively, and

[6] There are several possible basis functions with $c = (1, x, x^2, ..., x^p)$ furnishing one example on $\mathbb{R}$; see (2)

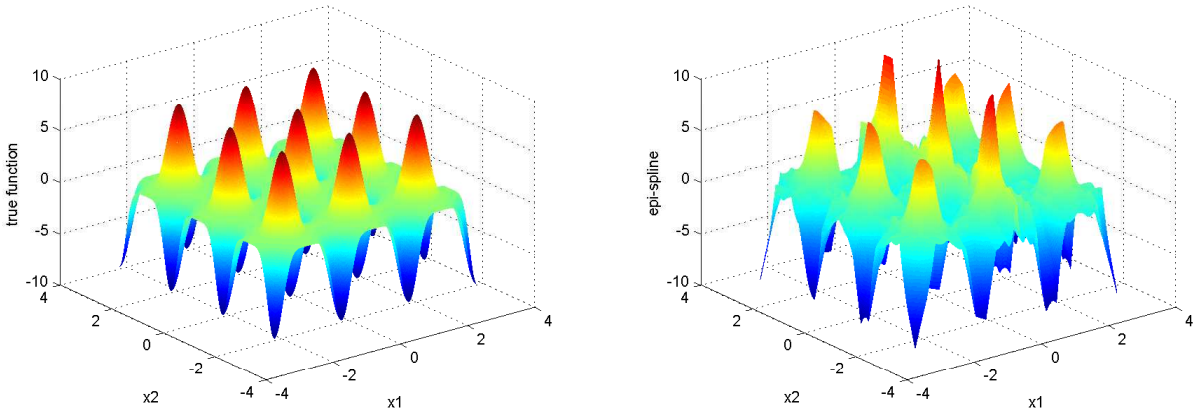

(a) (b)

Figure 13: Image reconstruction example: true function (a) and epi-spline (b).

$\bar{\psi}(r), \bar{\psi}^\nu(r^\nu) \geq -\rho_0$. Let $\rho > \rho_0$, $\rho' > \hat{dl}_\rho(R, R^\nu) + \rho$, and assume that $\bar{\psi}$, $\bar{\psi}^\nu$ are Lipschitz on $\rho' I\!B$ with constant κ. Then, for any $\varepsilon > 0$ and r^0 optimal in $(\bar{P})$,

$$d(r^0, \bar{R}^\nu_\varepsilon) \leq \left(1 + \frac{4\rho}{\varepsilon}\right) \left[\max_{r \in \rho B}\{\bar{\psi}(r) - \bar{\psi}^\nu(r)\} + (\kappa + 1)\hat{dl}_\rho(R, R^\nu)\right].$$

We observe that an error between an optimal solution of $(\bar{P})$ and $\bar{R}^\nu_\varepsilon$ originates from two sources: the differences between the criterion functions $\bar{\psi}$ and $\bar{\psi}^\nu$ and between the restrictions imposed through R and R^ν measured in terms of the $\hat{dl}_\rho$-distance, now defined for arbitrary sets and not only epi-graphs.

6 Examples

We provide numerical results for three gradually more complex examples. The first example estimates a common test function from image reconstruction. The second example estimates the probability density of simulation output. The third example forecasts electricity (load) demand on the basis of weather predictions.

Image reconstruction. We consider the standard test function $f(x) = (\cos(\pi x_1) + \cos(\pi x_2))^3$ defined on $[-3, 3]^2$; see Figure 13(a). We rely on continuous epi-splines and a partition of $[-3, 3]^2$ consisting of 20 by 20 squares so that $N = 400$. Based on 900 uniformly distributed data points and the max absolute error criterion, we obtain the epi-spline fit of Figure 13(b). Maximum and average errors across the data points are 0.415 and 0.313, respectively. Mean square and mean absolute error criteria give similar results. A relaxation of the continuity requirement results in essentially perfect interpolation at the expense of a more "rugged" fit.

Simulation output estimation. Estimates of the probability density function of the output of simulation model provide a comprehensive picture of the performance of the system modelled. Although kernel methods and other traditional methods of nonparametric statistics compute density estimates, they rely heavily on large-sample sizes and only in parts can account for external information, a prevalent factor in practical simulation studies. As laid out in [21], probability density estimation using epi-splines offers the possibility to include an arbitrary collection of external information and thereby achieve high-quality estimates even for small sample sizes.

For a sample $X^1, X^2, ..., X^\nu$ that is independently and identically distributed as a "true distribution," it is well-known (see for example [21]) that a constrained maximum likelihood estimator is an optimal solution of

$$\max \frac{1}{\nu} \prod_{i=1}^{\nu} h(X^i)^{1/\nu} \text{ such that } h \geq 0, \int h(x)dx = 1, h \in \mathcal{H},$$

where $\mathcal{H}$ is an appropriately selected space of functions on $\mathbb{R}^n$. Passing through the transformation $h = e^{-f}$, we arrive after equivalently maximizing the logarithm of the objective function at the problem

$$\min \frac{1}{\nu} \sum_{i=1}^{\nu} f(X^i) \text{ such that } \int e^{-f(x)}dx = 1, f \in \mathcal{F},$$

where, as above, we let $\mathcal{F} \subseteq$ lsc-fcns($\mathbb{R}^n$). Since this problem is infinite-dimensional, we formulate the approximate problem

$$\min \frac{1}{\nu} \sum_{i=1}^{\nu} s(X^i) \text{ such that } s \in F^\nu \cap \mathcal{S}^\nu$$

over epi-splines, where $\mathcal{S}^\nu =$ e-spl$_n^p(\mathcal{R}) \cap \mathcal{F}$, as above, and F^ν is a subset of functions satisfying $\int e^{-s(x)}dx = 1$, but also other restrictions derived from external information. A solution s of the approximate problem provides a density estimator through the composition e^{-s}, where we observe that the nonnegativity is automatically satisfied.

An example taken from [24] illustrates the possibilities. We consider an M/M/1 queue with arrival rate $\lambda = 1$ and service rate $\mu = 1.5$, but 50% of customers who enter the system are held at a separate station for two time units before entering the queue. We wish to estimate the density of the customer time-in-service (TIS). The true density is an equal mixture of the density corresponding to an M/M/1 queue without the holding station, which is exponential, and the same density shifted to the right by two time units. The resulting density is discontinuous at two time units as half the customers will have two time units added to their time in system; see the dotted line in Figure 14.

We assume that this detailed information about the density for customer TIS is unavailable and that we must rely on 100 simulated customer TIS as well as reasonable, external information. Of course, in practice this is the common situation. We build a second-order epi-spline estimate by solving the above approximate problem, under the external information that the customer TIS is nonnegative, derivatives

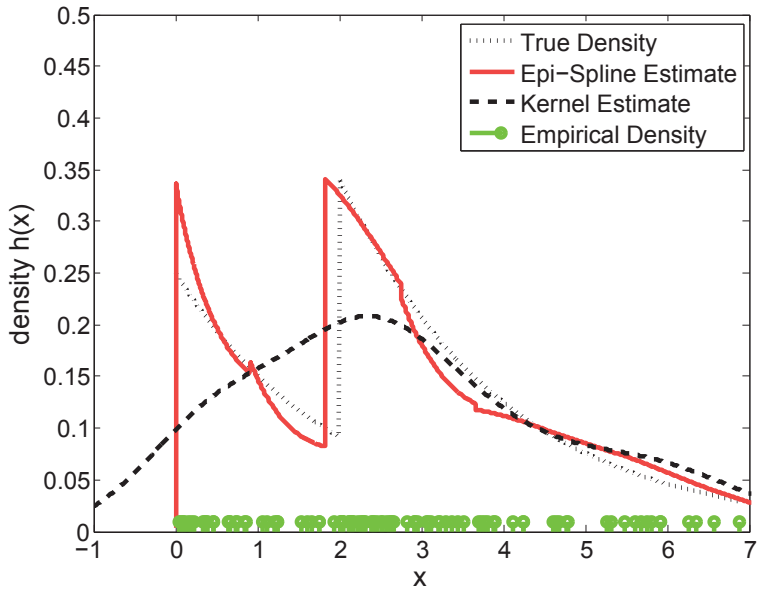

Figure 14: Density of queuing simulation.

relative to density values are bounded (i.e., a bound on the pointwise Fisher information), second-order derivatives are bounded, and the upper tail is log-concave. Using a mesh consisting of $N = 10$ intervals, we obtain the estimate given by the red line in Figure 14. The picture is representative of hundreds of draws of 100 simulated customer TIS. We also illustrate a standard gaussian kernel estimate. The green stems indicate the 100 simulated customer TIS. The estimate based on epi-splines tracks the true density closely and, in contrast to the kernel estimate, captures its essence. From this and similar examples in [24], we conclude that epi-spline technology provides a tool for analyzing simulation output under a variety of external information. In particular, flexibility of this kind is important when simulations are expensive and only a small sample can be made available. The burden then falls on the external sources to provide information that can sharpen performance estimates and support decision about the underlying system.

Electricity load forecast. A significant portion of electricity supply in the United States is provided through "day-ahead" contracts, where producers agree to deliver certain quantities of electricity for the next day. A central component of a market place for such contracts is forecasting tools for the next day's electricity load (demand). Such tools must necessary rely on the information available at the time of forecasting, which typically includes weather forecasts for the next day (temperature, dew point, cloud cover, etc.) as well as historical information about electricity load on days that had similar weather forecasts. Figure 15(a) shows temperature forecasts for five days in Boston in 2012, with corresponding actually observed electricity loads on those days shown in Figure 15(b). Although, the historical information may stretch decades back, the useful information is much more limited as the

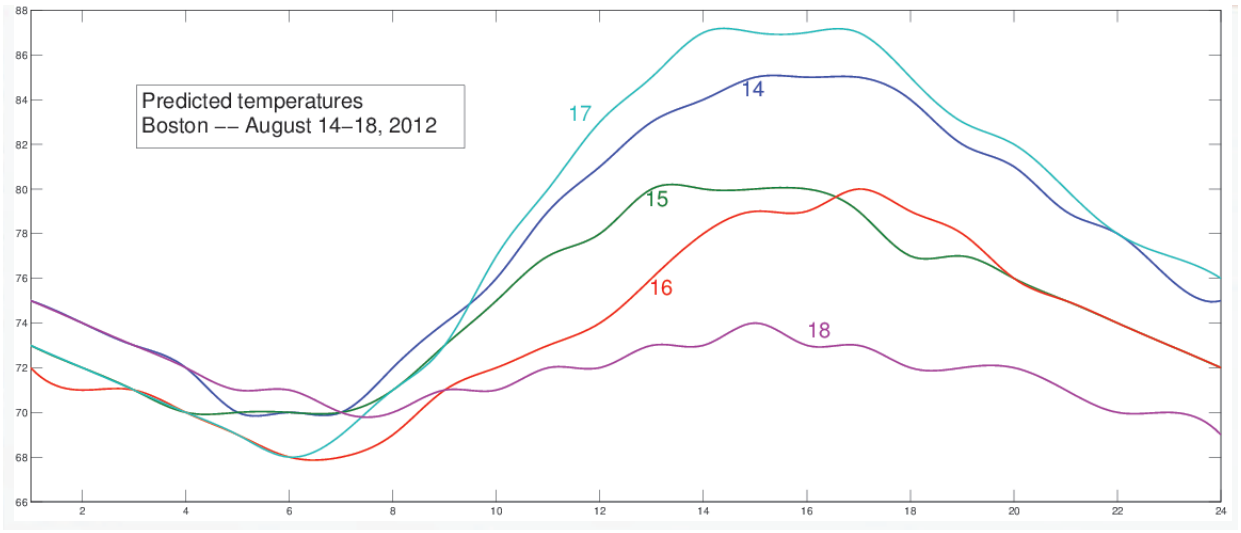

(a)

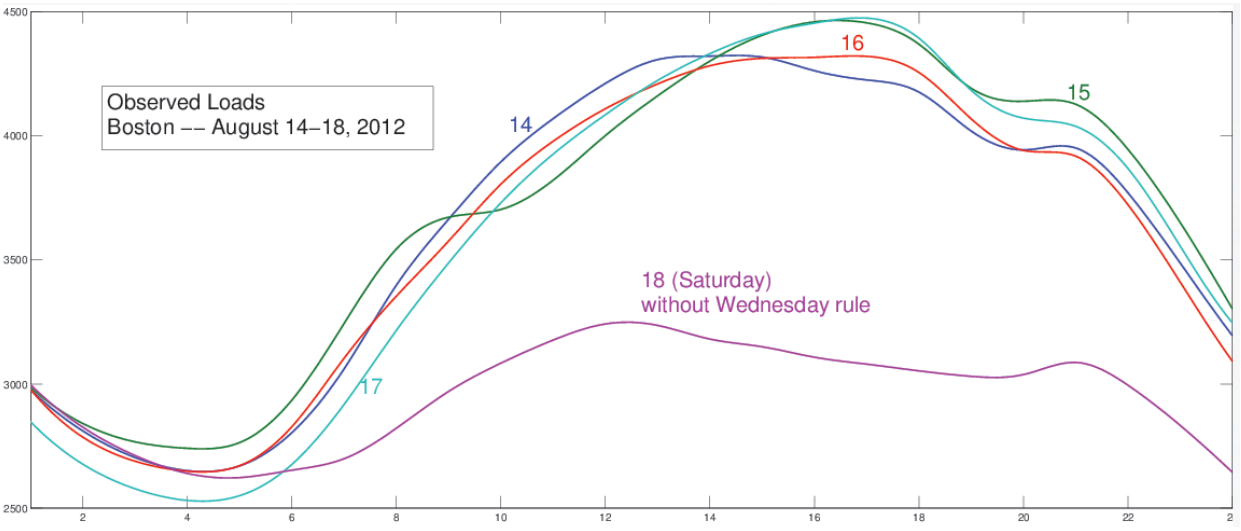

(b)

Figure 15: Temperature forecasts (a) and corresponding actual loads (b) for five days.

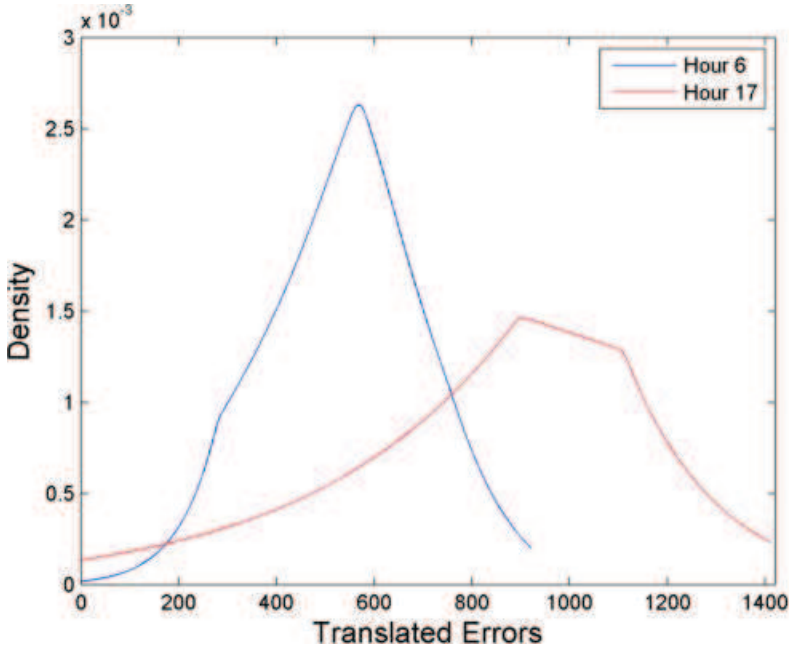

Figure 16: Probability densities of errors during two hours of the day.

data needs to be carefully segmented to ensure that only "similar" days are included; see [13, 14]. For examples, data for Mondays should not be mixed with those for Saturdays as the electricity load are fundamentally different on the weekend, and data for hot days should not be mixed with those of cool days. In the end, only about 15 to 25 days per year may remain and on which the forecast must rely making traditional techniques based on time-series or stochastic differential equations inaccurate. We here briefly describe the epi-spline-based construction of a stochastic process of the next day's electricity load as laid out in [13, 14], see also [16]. Epi-splines enter at three points. First, to help segment the data, probability density functions are estimated using an approach similar to that described for simulation output above. Second, a regression model builds an estimate of the "expected" load for the full 24 hours of the next day. Third, conditional probability density estimates quantify the variability in the process. We here describe the two last steps only.

Suppose that there are J days of historical data on which to base the estimates. For each day $j = 1, 2, ..., J$, and hour $h = 1, 2, ..., 24$, of that day, we know the forecasted temperature t_h^j, the forecasted dew point d_h^j, and the actually observed load l_h^j. Additional weather statistic is also available, but excluded here for simplicity of exposition. Anyhow, temperature and dew point forecasts appear to suffice for the estimation of summer days [13, 14]. The regression model then takes the form

$$l_h^j = s^{\text{tmp}}(h)t_h^j + s^{\text{dpt}}(h)d_h^j + e_h^j,$$

where s^{tmp} and s^{dpt} are epi-splines defined on $[0, 24]$ and e_h^j is the error between the observed load l_h^j and the predicted load $s^{\text{tmp}}(h)t_h^j + s^{\text{dpt}}(h)d_h^j$. We note that here the "coefficients" in front of the

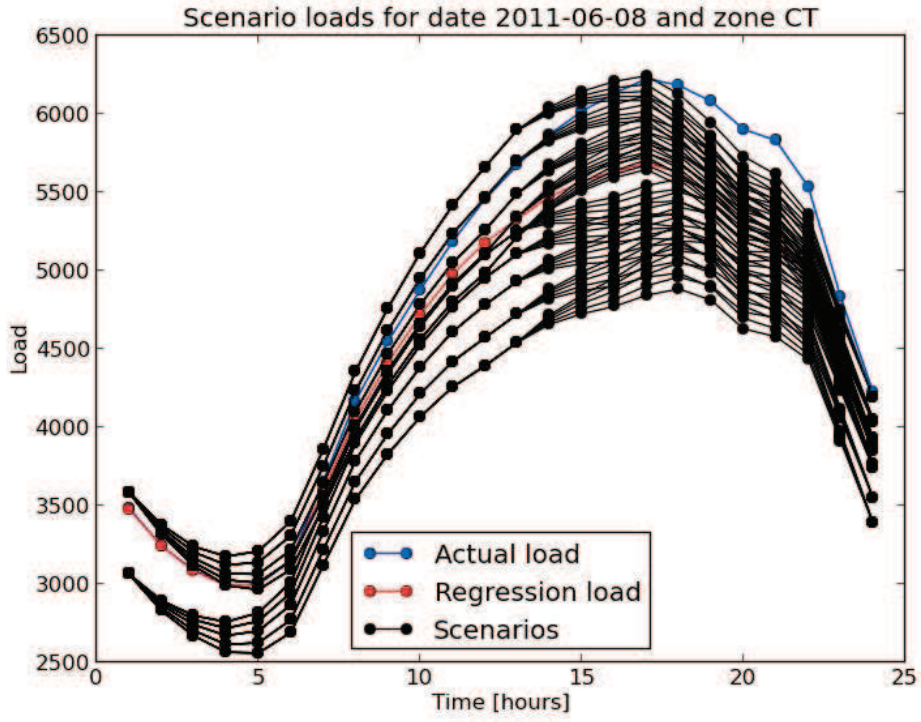

Figure 17: Regression load, with estimated uncertainty, and actual load.

explanatory variables "temperature" and "dew point" are functions of time. The regression problem is then to determine epi-splines s^{tmp} and s^{dpt} that

$$\text{minimize} \sum_{j=1}^{J} \sum_{h=1}^{24} \left| l_h^j - s^{\text{tmp}}(h) t_h^j - s^{\text{dpt}}(h) d_h^j \right|,$$

with the external information that the epi-splines are of second order, are continuously differentiable, and have bounded second-order derivatives. Using the representation of polynomials in (2) and mesh-points $m_k = k24/N$, $k = 1, 2, ..., N$, partitioning $[0, 24]$ into N intervals, we obtain that

$$s^{\text{tmp}}(x) = a_0^{k,\text{tmp}} + a_1^{k,\text{tmp}} x + a_2^{k,\text{tmp}} x^2, \quad \text{for } x \in (m_{k-1}, m_k),$$

with continuity forcing the epi-spline on the mesh-points to be defined by the values at the adjacent intervals; s^{dpt} is defined similarly in terms of parameters $a_0^{k,\text{dpt}}$, $a_1^{k,\text{dpt}}$, and $a_2^{k,\text{dpt}}$. Let $m_0 = 0$. The regression problem then takes the form of a linear program over those parameters as well as the auxiliary parameters z_h^j:

$$\min \sum_{j=1}^{J} \sum_{h=1}^{24} z_h^j \text{ such that}$$

$$l_h^j - (a_0^{k,\text{tmp}} + a_1^{k,\text{tmp}} h + a_2^{k,\text{tmp}} h^2) t_h^j - (a_0^{k,\text{dpt}} + a_1^{k,\text{dpt}} h + a_2^{k,\text{dpt}} h^2) d_h^j \le z_h^j, \quad h \in (m_{k-1}, m_k] \quad (3)$$
$$k = 1, ..., N, \ j = 1, ..., J$$

$$-l_h^j + (a_0^{k,\text{tmp}} + a_1^{k,\text{tmp}} h + a_2^{k,\text{tmp}} h^2) t_h^j + (a_0^{k,\text{dpt}} + a_1^{k,\text{dpt}} h + a_2^{k,\text{dpt}} h^2) d_h^j \le z_h^j, \quad h \in (m_{k-1}, m_k] \quad (4)$$
$$k = 1, ..., N, \ j = 1, ..., J$$

$$a_0^{k,\text{tmp}} + a_1^{k,\text{tmp}} m_k + a_2^{k,\text{tmp}} m_k^2 - (a_0^{k+1,\text{tmp}} + a_1^{k+1,\text{tmp}} m_k + a_2^{k+1,\text{tmp}} m_k^2) = 0, \quad k = 1, ..., N-1 \quad (5)$$

$$a_1^{k,\text{tmp}} + 2a_2^{k,\text{tmp}} m_k - (a_1^{k+1,\text{tmp}} + 2a_2^{k+1,\text{tmp}} m_k) = 0, \quad k = 1, ..., N-1 \quad (6)$$

$$-\kappa \le a_2^{k,\text{dpt}}, a_2^{k,\text{tmp}} \le \kappa, \quad k = 1, ..., N \quad (7)$$

The inequalities (3) and (4) linearize the criterion function, (5) and (6) ensure continuity and continuous differentiability requirements (see §3.3), and (7) bounds the magnitude of the second-order derivatives to κ. In [14], $N = 24$ and $\kappa = 500$. A slightly more complicated version with weighted errors is also possible.

The regression curve can be viewed as the drift of the stochastic process that forecasts the electricity load. The next step is to determine the volatility of the process. For a fixed hour h, we can interpret the minimized errors $\{e_h^j\}_{j=1}^J$ as the observations associated with the distribution of these errors. Using the epi-spline-based procedure for estimating probability densities described above, it is then possible to estimate this distribution. Since the number of observed errors will be limited, it becomes especially critical to include external information to ensure quality estimates. We can repeat this process for each hour h independently, but that would not take into account *conditioning*. Clearly, if the load at hour h is substantially higher than the load tentatively projected by the regression curve, one should take

this into account when looking at the distribution of the errors at a later time $h + \triangle h$. This can be done systematically by restricting the samples of the error at time $h + \triangle h$ to those that come from (observed) load trajectories that at time h had similar deviations from the overall drift of the process, i.e., from the regression curve; see [13, 14, 16] for details. Since this limits the number of data point on which a single density estimate must rely, the significance of being able to include external information in the epi-spline framework is further highlighted.

Extensive numerical results are provided by [13, 14] for cases studies covering the New England region of the United States. Figure 16 from [13] illustrates two epi-spline-based estimates of the probability density function of errors at hours $h = 6$ and 17 on a particular day. For a day with high variability in electricity load taken from [14], Figure 17 gives an example of estimated loads in 2011 in Connecticut according to the regression model (red line), the associated uncertainty given in terms of alternative scenarios (black lines), and the actual load (blue line). It is clear that the constructed stochastic process covers the true load to a high degree. Table 6 taken from [14] shows aggregated forecasting error statistics in terms of mean average percent forecasting errors from actual loads for different seasons and number of segments used in the procedure for segmenting the data into cluster of "similar" days. We find that regardless of the season, the forecasting errors are small, especially under an intelligent segmentation of the data. The epi-spline-based forecasting method of [13, 14] is currently being implemented by an independent software provider, with planned adoption by the New England Independent System Operator to support daily planning in 2014.

	Number of segments			
Season	1	3	5	7
Fall	5.45	4.66	4.2	3.99
Spring	3.1	2.88	2.67	2.73
Summer	10.25	4.82	4.14	4.19
Winter	5.25	3.32	3.29	3.47

Table 1: Mean average percent forecasting error in electric load forecast.

References

[1] M. Atteia. Généralisation de la définition et des propriétés de "splines-fonctions". *Comptes Rendus de l'Académie des Sciences de Paris*, 260:3350–3553, 1965.

[2] H. Attouch, R. Lucchetti, and R. Wets. The topology of the ρ-Hausdorff distance. *Annali di Matematica pura ed applicata*, CLX:303–320, 1991.

[3] H. Attouch and R. Wets. A convergence theory for saddle functions. *Transactions of the American Mathematical Society*, 280(1):1–41, 1983.

[4] H. Attouch and R. J-B Wets. Epigraphical analysis. In *Analyse Non Lineàire*, pages 73–100. Gauthier-Villars, Paris, 1989.

[5] H. Attouch and R. J-B Wets. Quantitative stability of variational systems: III. ε-approximate solutions. *Mathematical Programming*, 61:197–214, 1993.

[6] G. Beer. *Topologies on Closed and Closed Convex Sets*, volume 268 of *Mathematics and its Applications*. Kluwer, 1992.

[7] M. Casey and R. Wets. Density estimation: exploiting non-data information. Technical report, Mathematics, University of California, Davis, 2010.

[8] S. Chatterjee and P. Diaconis. Estimating and understanding exponential random graph models. *Annals of Statistics*, 41(5):2428–2461, 2013.

[9] H.B. Curry and I.J. Schoenberg. On spline distributions and their limits: The Polya distribution functions. *Bulletin of the American Mathematical Society*, 53:1114, 1947.

[10] H.B. Curry and I.J. Schoenberg. On Polya frequency functions IV: The fundamental spline functions and their limits. *Journal d'Analyse Mathématique*, 17:71–107, 1966.

[11] C. de Boer. Best approximation properties of spline functions of odd degree. *Journal of Mathematical Mechanics*, 12:747–749, 1963.

[12] M. Egerstedt and C. Martin. *Control Theoretic Splines*. Princeton University Press, 2010.

[13] Y. Feng, D. Gade, S. Ryan, J.-P. Watson, R. Wets, and D. Woodruff. A new approximation method for generating day-ahead load scenarios. In *Proceedings of the IEEE Power & Energy Society General Meeting*. IEEE, 2013.

[14] Y. Feng, I. Rios, S.M. Ryan, K. Spürkel, J.-P. Watson, R.J-B Wets, and D. Woodruff. Toward scalable stochastic unit commitment - part 1: Load scenario generation. In review, 2013.

[15] J.C. Holladay. A smoothest curve approximation. *Math. Tables Aids Comput.*, 11:233–243, 1957.

[16] I. Rios, R. Wets, and D. Woodruff. Multi-period forecasting and scenarios geneation with limited data. *Computational Management Science*, in review, 2014.

[17] R.T. Rockafellar and S. Uryasev. The fundamental risk quadrangle in risk management, optimization and statistical estimation. *Surveys in Operations Research and Management Science*, 18(1-2):33–53, 2013.

[18] R.T. Rockafellar and R. Wets. *Variational Analysis*, volume 317 of *Grundlehren der Mathematischen Wissenschaft*. Springer, 3rd printing-2009 edition, 1998.

[19] J.O. Royset, N. Sukumar, and R. J-B Wets. Uncertainty quantification using exponential epi-splines. In *Proceedings of the International Conference on Structural Safety and Reliability*, 2013.

[20] J.O. Royset and R. Wets. Epi-splines and exponential epi-splines: pliable approximation tools. pre-print, University of California, Davis, 2013.

[21] J.O. Royset and R. Wets. Fusion of soft and hard information in nonparametric density estimation. pre-print, University of California, Davis, 2013.

[22] J.O. Royset and R. Wets. Multi-dimensional epi-splines and their applications to infinite-dimensional optimization. pre-print, University of California, Davis, 2014.

[23] I. Schoenberg. Contributions to the problem of approximation of equidistant data by analytic functions. *Quaterly of Applied Mathematics*, 4(45-99, 112-141), 1946.

[24] D.I. Singham, J.O. Royset, and R. J-B Wets. Density estimation of simulation output using exponential epi-splines. In *Winter Simulation Conference*, 2013.

[25] R. Sood and R. Wets. Information fusion. http://www.math.ucdavis.edu/˜prop01, 2011.

[26] G. Wahba. *Spline Models for Observational Data*. SIAM, 1990.

[27] R. Wets and S. Bianchi. Term and volatility structures. In S. Zenios and W. Ziemba, editors, *Handbook of Asset and Liability Management*, pages 26–68. Elsevier, 2006.

[28] R. Wets, S. Bianchi, and L. Yang. Serious zero-curves. EpiRisk: http://epirisk.com/epicurves.php4, 2002.

[29] R. Wets and I. Rios. Modeling and estimating commodity prices: copper prices. *Mathematics of Finance and Economics*, in review, 2013.